

MetaML-Pro: Cross-Stage Design Flow Automation for Efficient Deep Learning Acceleration

ZHIQIANG QUE, Imperial College London, UK
JOSE G. F. COUTINHO, Imperial College London, UK
CE GUO, Imperial College London, UK
HONGXIANG FAN, Imperial College London, UK
WAYNE LUK, Imperial College London, UK

This paper presents a unified framework for codifying and automating optimization strategies to efficiently deploy deep neural networks (DNNs) on resource-constrained hardware, such as FPGAs, while maintaining high performance, accuracy, and resource efficiency. Deploying DNNs on such platforms involves addressing the significant challenge of balancing performance, resource usage (e.g., DSPs and LUTs), and inference accuracy, which often requires extensive manual effort and domain expertise. Our novel approach addresses two core key issues: (i) encoding custom optimization strategies and (ii) enabling cross-stage optimization search. In particular, our proposed framework seamlessly integrates programmatic DNN optimization techniques with high-level synthesis (HLS)-based metaprogramming, leveraging advanced design space exploration (DSE) strategies like Bayesian optimization to automate both top-down and bottom-up design flows. Hence, we reduce the need for manual intervention and domain expertise. In addition, the framework introduces customizable optimization, transformation, and control blocks to enhance DNN accelerator performance and resource efficiency. Experimental results demonstrate up to a 92% DSP and 89% LUT usage reduction for select networks, while preserving accuracy, along with a 15.6-fold reduction in optimization time compared to grid search. These results highlight the potential for automating the generation of resource-efficient DNN accelerator designs with minimum effort.

CCS Concepts: • **Hardware** → **Electronic design automation; Emerging tools and methodologies; Hardware-software codesign; • Computer systems organization** → **Neural networks; Reconfigurable computing.**

Additional Key Words and Phrases: FPGAs, algorithm-hardware codesign, design automation, design space exploration

ACM Reference Format:

Zhiqiang Que, Jose G. F. Coutinho, Ce Guo, Hongxiang Fan, and Wayne Luk. 2025. MetaML-Pro: Cross-Stage Design Flow Automation for Efficient Deep Learning Acceleration. *J. ACM* 1, 1, Article 1 (March 2025), 28 pages. <https://doi.org/10.1145/nnnnnnn.nnnnnnn>

1 INTRODUCTION

The field of deep learning has witnessed unprecedented growth in recent years, driven by the increasing demand for efficient and high-performance applications [20]. Consequently, FPGA-based deep neural network (DNN) accelerator design and optimization have gained significant

Authors' addresses: Zhiqiang Que, z.que@imperial.ac.uk, Imperial College London, UK; Jose G. F. Coutinho, gabriel.figueiredo@imperial.ac.uk, Imperial College London, UK; Ce Guo, Imperial College London, UK; Hongxiang Fan, Imperial College London, UK; Wayne Luk, w.luk@imperial.ac.uk, Imperial College London, UK.

Permission to make digital or hard copies of all or part of this work for personal or classroom use is granted without fee provided that copies are not made or distributed for profit or commercial advantage and that copies bear this notice and the full citation on the first page. Copyrights for components of this work owned by others than ACM must be honored. Abstracting with credit is permitted. To copy otherwise, or republish, to post on servers or to redistribute to lists, requires prior specific permission and/or a fee. Request permissions from permissions@acm.org.

© 2025 Association for Computing Machinery.

0004-5411/2025/3-ART1 \$15.00

<https://doi.org/10.1145/nnnnnnn.nnnnnnn>

attention [50, 52]. The development of an efficient FPGA-based DNN design requires a diverse skill set that combines expertise in machine learning with low-level knowledge of the target hardware architecture [36]. Optimizing these DNN designs is a complex process, as it involves balancing competing objectives. On one hand, high accuracy during inference is crucial from an application perspective. On the other hand, the design must be optimized for the underlying hardware architecture, meeting power, latency and throughput requirements while fitting into FPGA devices [5, 7]. Achieving an optimal balance between these conflicting objectives requires careful consideration and effective optimization strategies [44].

Existing optimization techniques for DNNs and hardware have a limitation in that they are often handled in separate stages, with information exchanged only in a top-down manner from the application to hardware. Bottom-up information flow, where hardware design insights inform DNN model optimization, typically requires manual intervention. However, this information exchange across multiple stages can significantly enhance the optimization process, as application and hardware optimizations can interact and affect each other. For instance, modifying the DNN model architecture could impact the FPGA resource utilization, and optimizing the FPGA design could influence the DNN model's accuracy [44]. In addition, there has been limited focus on combining optimization strategies targeting different abstraction levels, such as algorithmic level neural networks and High Level Synthesis (HLS) C++, hindering the selection of the most effective combination of optimization techniques for a given problem. In summary, few studies have thoroughly explored the vast configuration space that emerges when combining DNN optimization techniques across both software and hardware domains.

In this paper, we address these aforementioned technical challenges as follows:

- **C1. Custom Co-Optimization Strategies.** First, this work employs a unique co-optimization approach that refines both the DNN software model and the hardware architecture. By encoding software and hardware optimizations independently and composing them as needed, this approach enables modular reuse and adaptation of optimizations across different benchmarks and platforms. Through programmatic manipulation, it ensures tight coordination between DNN model and hardware-level optimizations, significantly expanding the design space and enhancing exploration capabilities.
- **C2. Cross-Stage Optimization Search.** Second, developing efficient DNN accelerators requires a coherent strategy that automates the selection, combination, and tuning of optimization techniques across multiple abstraction levels [2, 25, 48, 51]. It is challenging to identify the most effective combination, order and tuning of optimization techniques to ensure optimal outcomes [47, 52]. This work addresses these challenges by employing a cross-stage optimization search approach that coordinates the interaction between different stages of the design flow. By leveraging a combination of top-down and bottom-up optimization strategies, the framework dynamically adapts to the specific requirements of the hardware and the application, guiding the optimization process iteratively and identifying the best optimization techniques and their sequences.

Our proposed co-optimization framework, as illustrated in Fig. 1, operates across various computational spaces, such as software and High-Level Synthesis (HLS), and can potentially target diverse hardware platforms including FPGAs and ASICs (see C1). Each computational space represents an autonomous, custom optimisation task (e.g., OPT-1 to OPT-5, and potentially more), governed by tunable parameters. Moreover, this work utilizes a Bayesian [22, 32, 38] guided nested-loop optimization structure involving both local and global phases, combining very distinct optimization tasks and incorporating feedback from the latter stages of the design flow to refine the process iteratively (see C2).

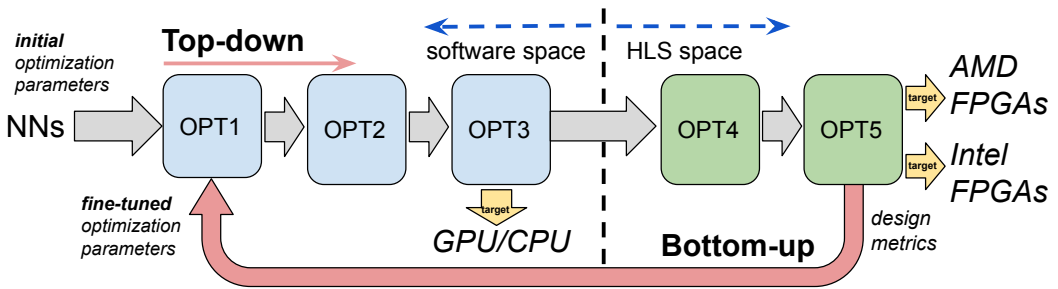


Fig. 1. The proposed approach.

We make the following contributions in this paper:

- A novel co-optimization framework that enables modular and adaptive hardware-software exploration for FPGA-based DNN accelerators. It independently encodes and combines optimizations for efficient design refinement. A cross-stage optimization search automates selection, ordering, and tuning across abstraction levels, dynamically adapting to hardware and application constraints through top-down and bottom-up strategies, ensuring efficient and high-performance designs (Section 3).
- A library of reusable optimization, transformation, and control tasks designed to be customizable and flexible, and that can be easily integrated into our co-optimization framework. This library includes optimization tasks such as pruning, quantization, and scaling to enhance DNN accelerator performance and resource efficiency. Moreover, we leverage metaprogramming to programmatically analyze and modify HLS C++ designs, enhancing design flexibility, performance tuning, and resource efficiency. In addition, we integrate Bayesian optimization to accelerate design space exploration while maintaining an optimal balance between accuracy and hardware efficiency. Some of the tasks in our library are specific to certain applications and target technologies, while others remain agnostic, providing versatility and adaptability within the framework (Section 4).
- A comprehensive evaluation of the proposed framework using multiple benchmarks and different optimization strategies. This evaluation provides insights into the effectiveness of the framework and its optimization modules under different scenarios (Section 5).

To the best of our knowledge, this is the first automated framework that combines reusable optimization components with adaptive feedback and global exploration to jointly balance resource efficiency and accuracy in deep learning designs.

Relationship to Prior Publications. This paper expands on our previous studies [27, 28, 31] which primarily focus on local optimizations. In [28], we propose MetaML, an optimization framework, that customizes design flow for DNNs with local optimizations. In [27], we introduce control capabilities within the optimization framework, while [28] focuses on Quantization Heuristic Search (QHS) optimization task for compressing DNN accelerators. However, these prior studies are limited in their ability to perform global optimization due to their focus on isolated optimization tasks. The inability to account for interdependencies between optimization tasks across stages mean that the overall design might not have achieved the optimal balance between accuracy, performance, and hardware resource. This work addresses these limitations by incorporating bottom-up feedback and leveraging Bayesian optimization to enable global optimization across the entire design flow. By adjusting optimization tasks at each stage based on performance feedback, our framework ensures that each optimization choice contributes to a more cohesive and globally optimal solution. This extended approach maintains high accuracy while improving resource

efficiency, specifically in resource-constrained environments. We plan to open-source MetaML-Pro to the research community, aiming to inspire further research and development in this area.

2 RELATED WORK

The field of FPGA-based DNN acceleration has rapidly expanded, leading to the development of numerous optimization techniques and tools. Several co-optimization techniques have been proposed that optimize both algorithm and hardware stages for DNNs on FPGAs, as discussed in various papers [6, 11–15, 17, 48, 51] and in hardware-aware neural architecture search studies like [2, 8, 25]. While hardware-aware neural architecture search (HW-NAS) approaches typically involve a holistic approach where the search algorithm must consider both software and hardware aspects together, often requiring a broader range of expertise within both NAS and hardware, our work modularizes the optimization process, allowing domain experts to focus on their areas of expertise. In addition, this modular design allows for individual optimization tasks to be reused independently in different contexts or different models, while the holistic nature and tight coupling of HW-NAS makes it challenging to reuse parts of the optimization process independently. This work can independently update and refine specific modules without affecting the entire system, resulting in better reusability and adaptability.

Other approaches offer end-to-end software frameworks, such as Xilinx’s Vitis AI [18] and Intel’s OpenVINO [1], which optimize DNNs with pre-built optimizations for deployment on specific target technologies. However, they are not designed for easy addition of new optimization strategies or to search for the most effective combined strategies.

Furthermore, some frameworks allow developers to describe and customize DNN optimization strategies, but their scope is limited. For instance, ScaleHLS [49] and SOTA-OPT [3] focus on HLS-based optimization strategies and hardware designs, but their optimization scope is restricted to MLIR. TVM [4] is a general-purpose DNN compilation framework that offers performance portability across different types of devices, but optimizations occur solely at the graph (IR) level.

Moreover, frameworks, such as FINN [40], HLS4ML [7], and fpgaConvNet [43], provide optimized hardware building blocks for FPGA-based DNN accelerators, and allow optimization strategies to be codified using these blocks. However, they do not support automated bottom-up optimization flows, where hardware stage information guides the optimization of the application (DNN) stage.

To overcome the limitations of existing optimization techniques for DNNs and hardware, our framework provides fully automated high-level optimization flows backed by reusable target-specific and target-agnostic building blocks. More specifically, our approach enables automated top-down and bottom-up flows, allowing for the creation of customized cross-stage optimization strategies for various DNN designs. Moreover, our approach integrates new and existing optimization techniques targeting various levels of abstraction, such as neural networks through graph optimizations and HLS C++ through source-to-source optimizations [42].

3 OUR APPROACH

3.1 Overview

In this paper, we introduce a novel framework for creating customizable design-flows that optimize FPGA-based DNNs, with a focus on automating both top-down and bottom-up flows between application and hardware optimization stages.

A design-flow represents a sequence of tasks that convert a high-level specification into a final hardware design. A design-flow is typically implemented as a multi-stage pipeline, with each stage operating on a specific model abstraction. As the pipeline progresses, the model abstraction is gradually reduced and optimized, taking into account the features of the target device. For example,

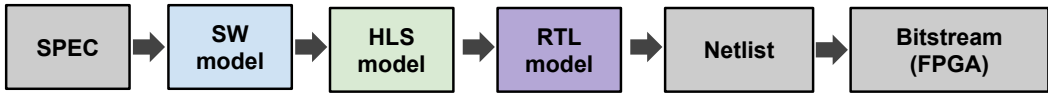


Fig. 2. A typical FPGA design flow. This FPGA design flow begins with defining the specifications (SPEC), followed by implementing and testing the design in software (SW). If High-Level Synthesis (HLS) is used, high-level code (e.g., C/C++) is converted into hardware description language (HDL). The design then moves to the Register Transfer Level (RTL) stage, where it is described in HDL (e.g., Verilog/VHDL) and synthesized into a netlist of logic gates. Finally, the netlist is used to generate a bitstream, which is loaded onto the FPGA to configure the hardware. Each stage progressively refines the design from concept to implementation.

a typical design-flow targeting FPGAs is shown in Fig. 2. It begins with defining specifications (SPEC) and testing the design in software (SW). If High-Level Synthesis (HLS) is used, a high-level DNN model, such as one described in TensorFlow, can be translated into a C++ HLS model using tools like HLS4ML. This model is then converted into an RTL description (e.g., Verilog/VHDL) using tools like Vivado HLS. The RTL model is further synthesized into a netlist, which is optimized for the FPGA’s architecture, and finally translated into a bitstream that configures the FPGA hardware.

Feedback information can be utilized to enable lower-stage information to refine higher-stage optimizations, employing more accurate metrics that were previously unavailable. We have developed a framework that allows users to codify fully automated optimizing design-flows with the following requirements:

- **Customizable:** Refers to the ability for users to customize, extend, or modify the design-flow to meet specific needs and support experimentation. Users can select a set of building tasks that implement optimization, transformation, or control tasks, combine them in a specific order, and fine-tune their parameters to generate a specific optimization flow. Additionally, they can create their own tasks and integrate them into their design-flow (see C1);
- **Multi-level:** Refers to the scope of optimizations and the ability to target multiple levels of abstraction, typically associated with different stages of a design-flow. For instance, optimizations operating at the Neural Network level are performed at the graph-level, while optimizations at the HLS C++ level are performed using source-level transformations (see C1);
- **Cross-stage:** Refers to the capability of a design-flow to support top-down and bottom-up flows between optimization stages, such as software and hardware, respectively (see C2).

This work focuses on custom optimizations in the SW and HLS stages while using default configuration for the remaining stages, however, the same concepts can be extended to the other stages, which is left for future work.

3.2 Architecture

Fig. 3 illustrates the key architectural components of a programmatically generated design flow using our approach, which comprises two main components: the pipe task and the meta-model.

The pipe task is the fundamental building block of the design flow and is responsible for implementing specific a task, such as optimization or control. By connecting pipe tasks, we create a complete design flow. The design flow’s internal architecture is represented by a cyclic directed graph, where nodes represent tasks, and edges represent **paths** between tasks. A path represents a dependency between two tasks, such that a task can only be executed if its dependencies have finished executing.

The meta-model, on the other hand, is responsible for storing all of the design flow’s states, including the configuration parameters of each pipe task and their respective outputs. Instead of communicating directly with each other, pipe tasks share information through the meta-model,

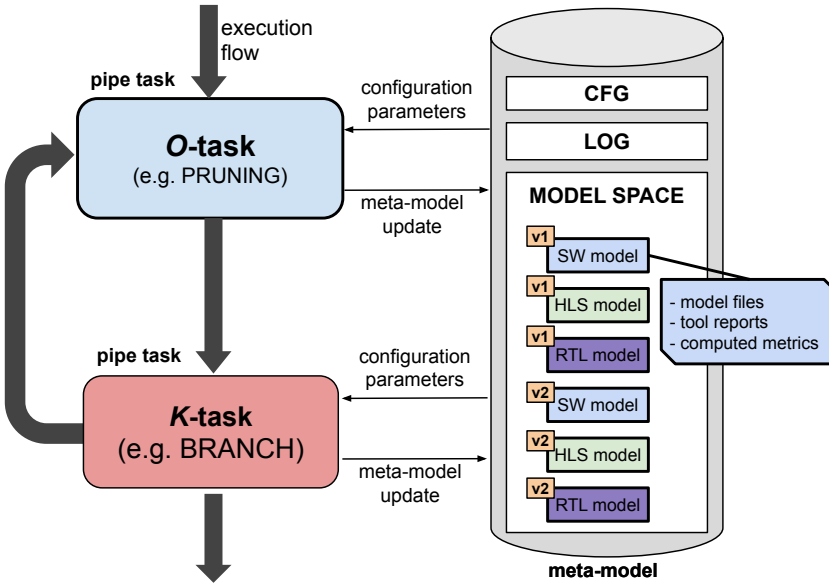


Fig. 3. A connection between a *O*-task and a *K*-task. A pipe task has a uniform interface allowing any two pipe tasks to be connected (although there may be constraints about how many connections a task can handle). A *O*-task typically enhances DNN models based on specific objectives and constraints. A *K*-task on the other hand, manages the control flow. Each connection defines a unidirectional stream between a source task and a target task.

which serves as a shared space. The meta-model has three sections, as illustrated in Fig. 3(b): configuration, log and model space.

The configuration section (**CFG**) is a key-value store that keeps the parameters of all pipe tasks in the design flow. These parameters can configure all pipe tasks of the same type or specific instances, and they can be supplied by the user or automatically modified by the pipe tasks as part of an automated tuning process. The log section (**LOG**) stores the runtime execution trace of the design flow. This section can be useful for debugging and understanding the execution flow of the design.

Finally, the **model space** stores the models generated during the execution of a design flow. Each stored model is versioned, and models derived by different stages can coexist in the same model space. In the example shown in the figure, we have stored six models covering three abstraction levels: DNN, HLS C++ , and RTL. Each model in the model space encapsulates all its supporting files, tool reports, and computed metrics. Moreover, they can be accessed and manipulated by any pipe task in the design flow, enabling cross-stage optimizations.

3.3 Reusable Pipe Tasks

Table 1 presents a list of pipe tasks that have been implemented in our approach, along with their roles, multiplicity, and parameters. The multiplicity denotes the number of input and output channels that a task can handle. We classify pipe tasks into three types based on their roles:

- **K-task**: These are generic tasks that control top-down and bottom-up flows. Examples include: **BRANCH**, which selects an output path at runtime based on a boolean condition; **JOIN**, which merges multiple paths into one; **FORK**, which allows multiple concurrent strategy paths; **REDUCE**, which consolidates the results of multiple strategy paths into one; and **STOP**, which terminates the design flow;

Table 1. A list of implemented pipe tasks.

Type	Role	Multiplicity	Parameters
JOIN	K	many-to-1	-
BRANCH	K	1-to-2	fn: meta-model \rightarrow bool
FORK	K	1-to-many	-
REDUCE	K	many-to-1	fn: [meta-model] \rightarrow meta-model
STOP	K	1-to-0	fn: meta-model \rightarrow output
HLS4ML	λ	1-to-1	default_precision IOType FPGA_part_number clock_period test_dataset
VIVADO-HLS	λ	1-to-1	project_dir
INTEL-oneAPI	λ	1-to-1	project_dir
KERAS-MODEL -GEN	λ	0-to-1	train_en train_test_dataset train_epochs
PRUNING	O	1-to-1	tolerate_acc_loss (α_p) pruning_rate_thresh (β_p) train_test_dataset train_epochs
SCALING	O	1-to-1	default_scale_factor tolerate_acc_loss (α_s) scale_auto max_trials_num train_test_dataset train_epochs
QUANTIZATION	O	1-to-1	tolerate_acc_loss (α_q) train_test_dataset

- **O -task:** These are self-contained optimizing tasks that enhance deep learning models based on specific objectives and constraints. Our current pipe task repository includes PRUNING and SCALING, which are implemented using the Keras API (version 2.9.0), and QUANTIZATION, which is performed using C++ source-to-source transformations via the Artisan framework [42];
- **λ -task:** These tasks perform functional transformations on the model space, such as compilation and synthesis. Examples include HLS4ML (version 0.6.0), which translates a DNN model into an HLS C++ model, and Vivado HLS (version 20.1), which translates an HLS C++ model into an RTL model.

It is worth noting that our framework is customizable, allowing users to create and integrate their own pipe tasks tailored to their specific needs.

```

1 # The pruning strategy architecture - Fig. 2(a)
2 from MetaML import *
3 # design-flow architecture
4 with Dataflow() as df:
5     join = Join() << KerasModelGen()
6     branch = Branch('B') << (VivadoHLS() <<
7         (HLSML() << (Pruning() << join)))
8
9     branch >> [join, Stop()]
10 # design-flow configuration
11 cfg = {
12     'KerasModelGen::train_en': False,
13     'Pruning::tolerate_accuracy_loss': 0.02,
14     'Pruning::pruning_rate_threshold': 0.02,
15     'B@fn': lambda metamodel: ...
16     'HLS4ML::default_precision': 'ap_fixed<18,8>',
17     'HLS4ML::IOType': 'io_parallel',
18     'HLS4ML::FPGA_part_number': 'xc7z020clg400-1',
19     'HLS4ML::clock_period' : 10,
20     'train_test_dataset': '/mypath/target_dataset',
21     'train_epochs': 15,
22     'Stop::fn': lambda metamodel: ...
23 }
24 # run design-flow
25 optimised_model = df.run(cfg)

```

Listing 1. The implementation of the pruning strategy using our framework.

3.4 Building a Strategy

Listing.1 provides the Python code for implementing the pruning strategy depicted in Fig.8(a) and discussed in Section 5.2. The code consists of three sections: **(i)** lines 4–9 builds the design-flow architecture graph by connecting the corresponding tasks. The `>>` and `<<` operators are utilized to define the connections between task instances, and the default name of each task instance serves as its identifier, although it can be overridden by providing it as an argument (line 6). The end result is a cyclic-directed graph. **(ii)** lines 11–23 define the configuration object, which holds all the parameters for configuring the tasks. Parameters referred to as `TaskType::parameter` are passed to all tasks of that task type (lines 16–19), whereas parameter names in the format of `InstanceName@parameter` are passed to a specific instance (line 15). All other parameters are global (lines 20–21) and accessible to any task. Finally, **(iii)** line 25 executes the design-flow by passing the configuration object.

The execution of the design-flow starts with graph validation, which ensures that there is at least one source task and no multiplicity constraints are violated. Tasks are executed by an internal scheduler using a thread pool, which assigns jobs to available workers or stalls until a worker becomes available. After validating the architecture graph, an empty meta-model is generated using the supplied configuration, and the scheduler runs the source task. When a task completes execution, it submits a job to execute the next set of tasks in the flow. The STOP task terminates execution when all submitted jobs are completed. Modifying the design-flow architecture and updating its configuration parameters can lead to new optimization strategies, which is discussed next.

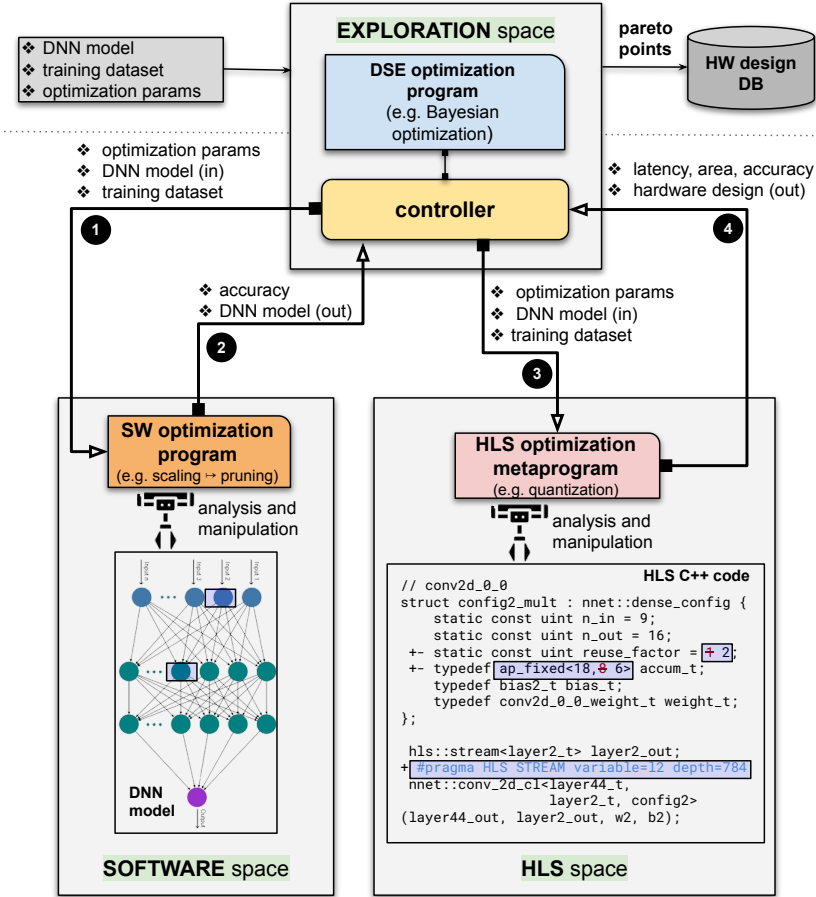


Fig. 4. This figure illustrates the implementation of our co-optimization framework, featuring an organized system of optimization spaces, each autonomously running Python programs within dedicated environments, overseen by an exploration space executing a general optimization strategy. The diagram depicts the orchestration of local optimization spaces, such as software and hardware, through a controller process.

4 IMPLEMENTATION

4.1 Co-Optimization Workflow

As illustrated in Fig. 4, our co-optimization approach allows the encoding of optimizations across different models of computation - from software to hardware (see C1 in Section 1). At the top level, a DSE optimization program is employed (see C2), executing a comprehensive exploration strategy and overseeing local optimizations at two (or more) distinct levels of abstraction. At the software DNN level, optimizations are executed on the architecture using tools like Tensorflow or PyTorch. At the HLS DNN level, optimizations are conducted by modifying the HLS code automatically using metaprogramming. Optimizing DNN models across multiple abstraction levels, from software to hardware, leverages complementary strategies that address different bottlenecks within the system. Software optimizations prioritize algorithmic efficiency and reducing computational complexity, while hardware optimizations target improvements in throughput, latency, resource utilization and energy efficiency.

Our co-optimization workflow begins with the Exploration space. Here, a DSE program utilizes a DNN model, training data, and configuration parameters to conduct the exploration workflow. This process yields a variety of hardware designs with trade-offs in metrics such as performance and accuracy. A controller process orchestrates this exploration by managing communication between the DSE program and local optimization spaces. Prior to exploration, the DSE program sets up and deploys optimization programs within these spaces. Fig. 4 depicts two such spaces: one for software (SW) utilizing TensorFlow and another for HLS employing Vivado HLS. Each space optimizes the model according to selected strategies, such as pruning or quantization.

After system setup, the exploration loop commences. In each iteration: ❶ The DSE program dispatches the DNN model and a specific parameter set to the software optimization space, where tasks like scaling and pruning are executed. ❷ Upon optimization completion, the refined model is returned to the controller along with its associated accuracy. ❸ Subsequently, the model is forwarded to the HLS space for additional optimization. A metaprogram adjusts the source code based on recommended optimizations (e.g., quantization) and parameter values from the controller. After synthesis, metrics such as power, area, and accuracy are obtained and ❹ fed back to the Exploration space. The DSE program evaluates designs using these metrics, retains promising candidates, and suggests new parameters for the next iteration.

This separation of concerns into distinct optimization spaces—software, HLS, and DSE—allows for the integration of diverse optimization strategies and techniques. It enables the introduction of faster or more effective exploration methods without altering existing optimizations. In addition, it combines exploration across software and hardware domains to identify effective techniques for optimizing performance. Moreover, it facilitates specialization of new hardware optimizations specific to certain FPGA HLS tools by allowing HLS code to be customized through metaprogramming.

4.2 Auto-Pruning with Binary Search

Pruning is a technique that improves the performance and efficiency of neural networks by removing insignificant weights. The pruning strategy uses a PRUNING *O*-task, which gradually zeroes out weights during training to create a more compact and efficient network while maintaining accuracy. This optimization task supports auto-pruning, which automatically determines the highest pruning rate while maintaining a given level of accuracy loss. The PRUNING *O*-task is illustrated in Fig. 8(a). Formally, the objective of this *O*-task is defined as:

$$\begin{aligned} & \text{maximum } Pruning_rate \\ & \text{subject to } Accuracy_loss(Pruning_rate) \leq \alpha_p \end{aligned} \quad (1)$$

Starting at 0% pruning rate, the auto-pruning algorithm obtains initial accuracy Acc_{p0} at step 1 (s_1). It then uses a binary search approach, increasing or decreasing the pruning rate based on whether the accuracy loss is within a user-defined tolerance ($\leq \alpha_p$) as shown in Table 1. The algorithm terminates when the rate difference is below a threshold (β_p). The number of steps is determined by $1 + \log_2(1/\beta_p)$. Algorithm search steps and direction are shown in Fig. 9. Both the tolerance ($\leq \alpha_p$) and threshold (β_p) values are initially set to 2% in this work.

4.3 Auto-Scaling

To accommodate large DNN designs on FPGAs, we adopt the SCALING *O*-task that automatically reduces the layer size while monitoring the result accuracy loss, denoted by α_s . The objective of this *O*-task is formally defined as:

$$\begin{aligned} & \text{minimum } Scaling_factor \\ & \text{subject to } Accuracy_loss(Scaling_factor) \leq \alpha_s \end{aligned} \quad (2)$$

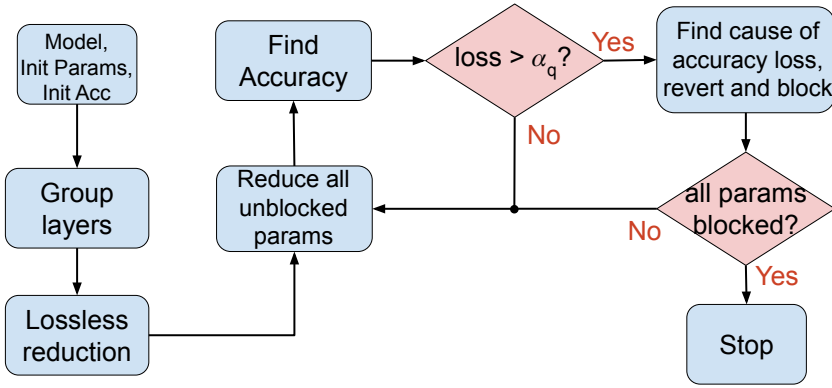


Fig. 5. The proposed QHS algorithm

The auto-scaling process begins with a scaling factor of 1 (i.e., no scaling), getting initial accuracy Acc_{s0} at step 1 (s1). The algorithm then gradually reduces the scaling factor, continuing the search until the accuracy loss exceeds the threshold α_s . If necessary, α_s can be adjusted to achieve further size reduction with minimal impact on accuracy.

4.4 Auto-Quantization with Heuristic Search

In our framework, we introduce quantization task based on the Quantization Heuristic Search (QHS) algorithm [31]. It automatically determines the lowest bitwidth for each layer while maintaining a given level of accuracy loss. Formally, the objective of this task is defined as:

$$\begin{aligned} & \text{maximum} && \textit{Bit_width_reduction} \\ & \text{subject to} && \textit{Accuracy_loss}(\textit{Bit_width_reduction}) \leq \alpha_q \end{aligned} \quad (3)$$

It performs mixed-precision quantization for DNNs, allowing separate precisions for the weights, biases and results of layers of a model, taking the advantages of the customizability of FPGAs. While this customizability creates a massive search space of quantization configurations, dependencies within the network can be used to reduce the degrees of freedom of the design space.

Fig. 5 shows the steps of the proposed QHS algorithm. The optimization task begins by accepting a model with a maximum tolerable accuracy loss, denoted as α_q . Initially, virtual layers are created, and lossless reduction is performed by minimizing the integer bits representing model parameters using the base-2 logarithm of the largest weight and bias in each layer, plus one bit for the sign to avoid saturation. Subsequently, all parameters (weights, biases and results) are initially assumed to be further reducible. The total bit-widths of these parameters are then reduced by one bit if they are considered reducible. This quantization is applied to the C++ kernel, and the accuracy is evaluated through a runtime simulation. If the accuracy loss remains within the user-specified tolerance, α_q , this step is repeated. If the accuracy loss exceeds the tolerance, the algorithm identifies and blocks non-reducible precisions. It determines which precisions are most sensitive by testing the reduction impact on accuracy. If a bit-width reduction breaks the accuracy constraint, that precision is marked non-reducible. The process repeats until no further reductions are possible within the accuracy constraints.

4.5 Metaprogramming for HLS Design Optimization

A novel aspect of our co-optimization approach is the integration of metaprogramming into hardware design optimization. In this section, we describe its key motivation and benefits, and how we integrate metaprogramming in our co-optimization framework.

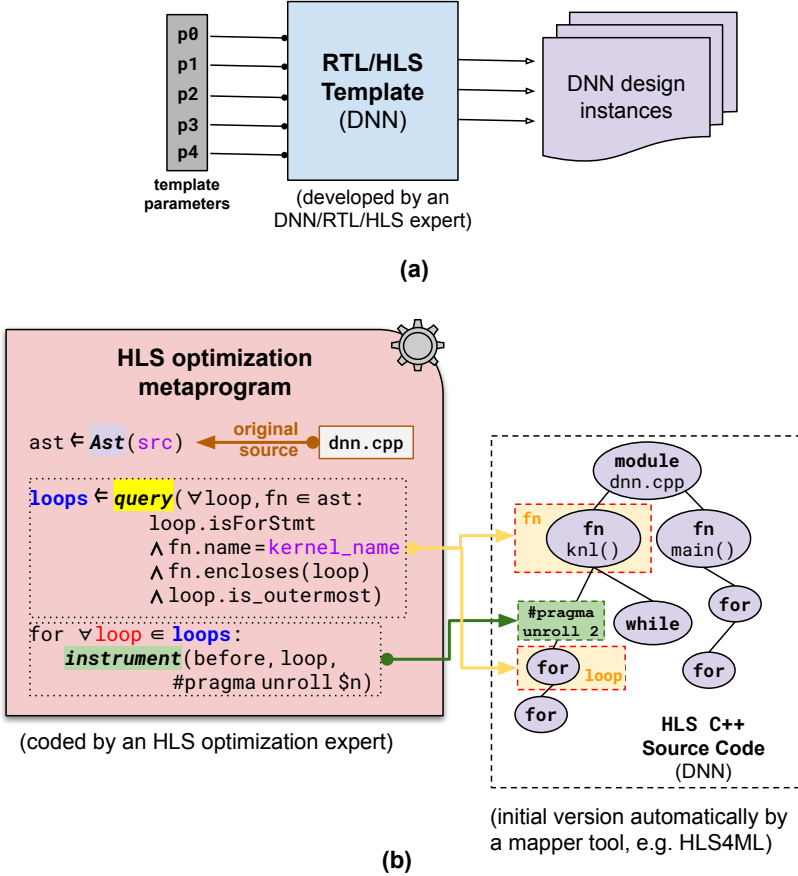


Fig. 6. (a) Current methods for deriving hardware designs rely on templates developed by experts. However, these templates are constrained in generating a finite number of design variants from predetermined parameter values and demand expertise for accommodating new DNN architectures. (b) An HLS metaprogram in pseudocode illustrating dynamic C++ code manipulation through Abstract Syntax Tree construction to derive an optimized design variant.

Limitations of template-based approaches. Traditional FPGA-based DNN acceleration frameworks typically rely on manually crafted templates to generate hardware designs. These templates encode expert knowledge, ensuring optimized implementations for a given set of parameters as illustrated in Fig. 6(a). However, they impose inherent limitations in flexibility, adaptability, and scalability. First, templates generate only a limited number of design variants by adjusting predefined parameters, restricting design exploration. They are optimized for specific architectures and are not easily generalizable to new DNN models or hardware platforms.

Extending these templates to support new DNN architectures requires deep domain knowledge in hardware design, making the process resource-intensive. Hardware engineers must manually introduce modifications, which increases development time and effort. Additionally, the modifications are constrained to specific parameterized components, preventing broader architectural transformations that might be necessary for emerging hardware and application demands. As a result, template-based methods struggle to efficiently explore the vast design space available in FPGA-based DNN acceleration.

Benefits of metaprogramming. Our metaprogramming approach addresses these challenges by dynamically analyzing and modifying HLS C++ source code using Python. This technique allows greater flexibility in exploring hardware optimization strategies. One key advantage is the ability to automate the insertion and tuning of HLS pragmas, such as loop unrolling and pipelining, without requiring manual intervention. By adjusting these pragmas dynamically, the hardware implementation can be fine-tuned for improved performance and resource utilization.

Additionally, metaprogramming facilitates code restructuring to improve computational efficiency and reduce design complexity. By programmatically modifying code, redundant computations can be eliminated, and data dependencies can be optimized. Another important capability is automated data type adjustments for quantization, which optimize memory footprint and computational precision by dynamically adapting numerical representations. Unlike static templates, which rely on predefined precision settings, metaprogramming can analyze the computational requirements of different layers and assign appropriate precision dynamically.

Another significant benefit is the incorporation of specialized FPGA libraries [41], enhancing performance for target platforms. By integrating device-specific optimizations at the source-code level, our approach ensures that the generated hardware designs are optimized for the underlying FPGA architecture. This adaptability makes metaprogramming a powerful tool for hardware-aware DNN optimization.

Example of an HLS metaprogram. Fig. 6(b) illustrates an HLS metaprogram that dynamically modifies a given C++ source file. The process begins with the construction of an Abstract Syntax Tree (AST) representation of the C++ code. The AST provides a structured representation of the source code, allowing precise modifications for any of its constructs. The metaprogram then performs code querying and analysis to identify outermost loop structures within kernel functions. These loops are critical for performance optimization, as their execution directly impacts resource utilization and latency.

Once the relevant loops are identified, the metaprogram instruments the code by inserting pragma directives such as `#pragma unroll $n`. These directives control loop unrolling dynamically, enabling optimized parallel execution of computations. By automating this process, the metaprogram allows rapid exploration of different optimization strategies without requiring manual code modifications. This automation significantly improves both efficiency and design flexibility, making it easier to adapt to different DNN architectures and FPGA platforms. A more detailed explanation about querying and instrumentation capabilities can be found in [42].

Application in quantization optimization. We integrate Quantization Heuristic Search (QHS), detailed in Section 4.4, as an optimization task within our framework using metaprogramming to refine fixed-point numerical representations directly at the HLS C++ level. As illustrated in Fig. 7, we develop a metaprogram called H4ML-API, which programmatically analyzes and modifies HLS4ML-generated code to automate the quantization process.

The workflow proceeds as follows. First, the HLS4ML tool generates an initial, unoptimized firmware from a DNN model. Then, ① the H4ML-API metaprogram inspects the source structure and executes the firmware to extract DNN architecture details, layer characteristics, and accuracy metrics. This information is ② passed to the QHS process, which identifies opportunities for bit-width reduction while maintaining model accuracy, dynamically adjusting bit-widths based on layer-specific requirements. The refined bit-width settings are then ③ transferred back to the H4ML-API, which ④ modifies the HLS C++ code accordingly. This iterative process continues from step ① while the accuracy loss remains within the α_q threshold.

A key feature of this approach is the creation of virtual layers to optimize bit-width allocation. Rather than treating each operation separately, the metaprogram groups cascaded operations into logical units, enabling more effective quantization. For instance, if a convolutional layer produces

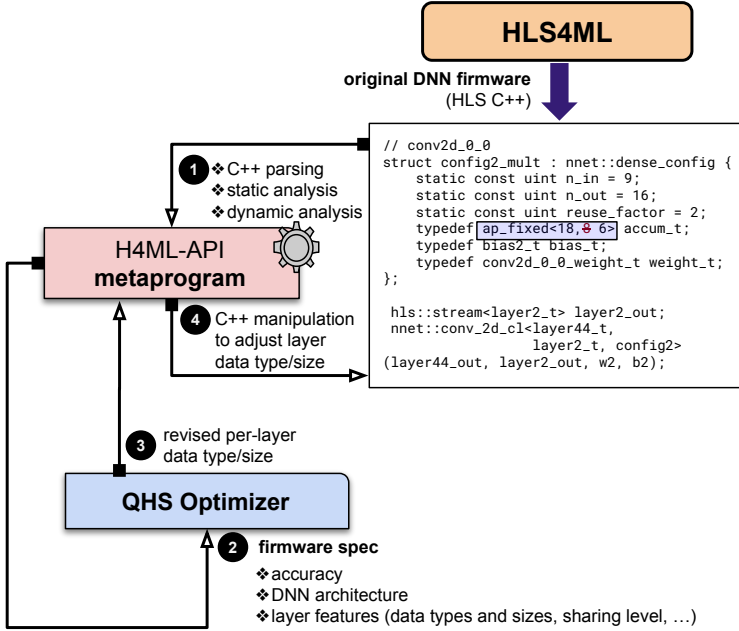


Fig. 7. Integration of the Quantization Heuristic Search (QHS) algorithm with HLS4ML and metaprogramming. The metaprogram dynamically adjusts data types and bit-widths at the HLS C++ level, optimizing computational efficiency while maintaining model accuracy.

an 8-bit output, subsequent operations such as max-pooling and batch normalization are assigned the same precision, avoiding redundant higher-bit computations. By systematically reducing bit-widths without compromising accuracy, this approach significantly decreases resource usage while maintaining high inference performance.

4.6 Design Space Exploration (DSE)

Within our approach, Design Space Exploration (DSE) algorithms are critical for automatically adjusting the optimization parameters in subsequent iterations to improve design performance, while maintaining high model accuracy and meeting the constraints of the device.

Bayesian optimization is a key algorithm we utilize for global optimization of expensive-to-evaluate functions (represented as $f(x)$). It models the objective function using a probabilistic model (e.g., Gaussian Process) and uses an acquisition function to decide where to sample next, balancing exploration of the design space with exploitation of known optimized configurations. In our context, x denotes the array of configuration settings, which serve as parameters for each optimization task within our framework. The process guides towards the most promising configurations for evaluation until a predetermined number of iterations is reached.

Our performance metrics encompass accuracy, hardware resource utilization, and adherence to operational constraints. We leverage hardware usage data obtained through Xilinx Vivado, including latency, DSP, LUT, FF, and BRAM, to inform our optimization strategy for model deployment, adjusting the optimization parameters including scaling, pruning, and quantization thresholds ($\alpha_{p/s/q}$). Due to the heterogeneity of these metrics, direct summation is impractical, necessitating normalization to standardize them. This normalization technique is widely applied in various DSE methods [35].

Table 2. Benchmarks used in this work

Model Name	Dataset	Application Domain
Jet-DNN [5, 7] / Jet-CNN	Jet-HLF [7]	Jet Identification (Particle Physics)
VGG-7 [34, 37]	MNIST [21]	Image Classification
ResNet-9 [10, 16]	SVHN [24]	Image Classification
LSTM [29]	MNIST	Sequence classification

Moreover, when optimizing a complex system, such as FPGA-based DNN accelerators, practical constraints must be considered. These constraints may arise from hardware limitations, performance requirements, and other critical factors. Incorporating these constraints into the Bayesian optimization process ensures that our search for the optimal solution occurs within a feasible and practical region of the design space. For hardware utilization constraints, a score becomes a negative maximum integer when the utilization is higher than a predefined threshold. This signals the Bayesian algorithm that the input parameter is unsuitable, steering the optimization away from poor configurations. The same approach applies to model accuracy constraint. The pseudocode of Bayesian score algorithm is shown below:

```

if (Bayesian constraints not met) then
     $f(x) = -sys.maxsize$ 
else
     $f(x) = \sum_{x \in \{Acc., DSP, LUT, BRAM\}} Norm\_Results[x] \times W[x]$ 

```

The algorithm assigns weights ($W[\text{metric}]$) to each metric to indicate their relative importance.

5 EVALUATION

In this section, we demonstrate how optimization strategies can be built by revising design-flow architectures, combining and reusing pipe tasks, and modifying their configuration (Sections 5.2 and 5.3). We explain flow control in Sections 5.6 and 5.5. We discuss optimisation search strategies and compare evaluation results with other approaches in Sections 5.7 and Section 5.10, respectively.

5.1 Experimental Setup

Experiments were conducted in Python 3.9.15 with benchmark workloads from typical DNN applications, as presented in Table 2), including jet identification [7, 23], image classification using VGG[34] and ResNet [16] networks. The jet identification task targeted FPGA-based CERN Large Hadron Collider (LHC) triggers with a 40 MHz input rate and a response latency of less than 1 microsecond. Default frequencies were 100MHz for Zynq 7020 and 200MHz for Alveo U250 and VU9P, and the HLS4ML task used 18-bit fixed-point precision with 8 integer bits.

5.2 Single O-task Strategies

In this subsection, we focus on three strategies which are backed by a single *O*-task each, respectively.

5.2.1 Pruning strategy. The effectiveness of the auto-pruning algorithm is demonstrated in Fig. 10. Figures (a) and (c) depict the pruning rate and accuracy for Jet-DNN and ResNet9 in each step, while (b) and (d) show the resources utilization on Zynq 7020 and U250. As the pruning rate increases, hardware resource requirements, particularly DSPs and LUTs, decrease, leading to improved FPGA performance. The design candidate with the highest pruning rate within the allowed tolerance is selected.

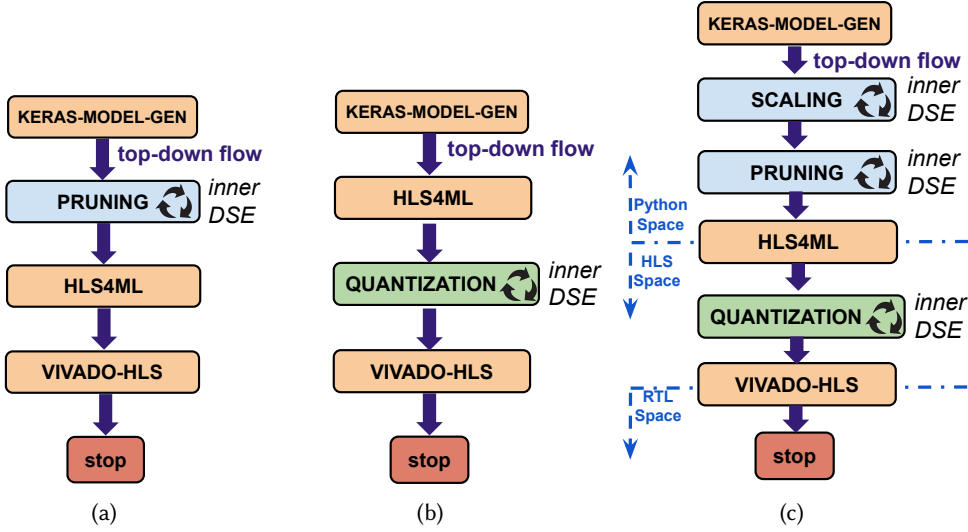


Fig. 8. (a) Pruning strategy. (b) Quantization strategy. (c) The combined strategy of scaling, pruning and quantization.

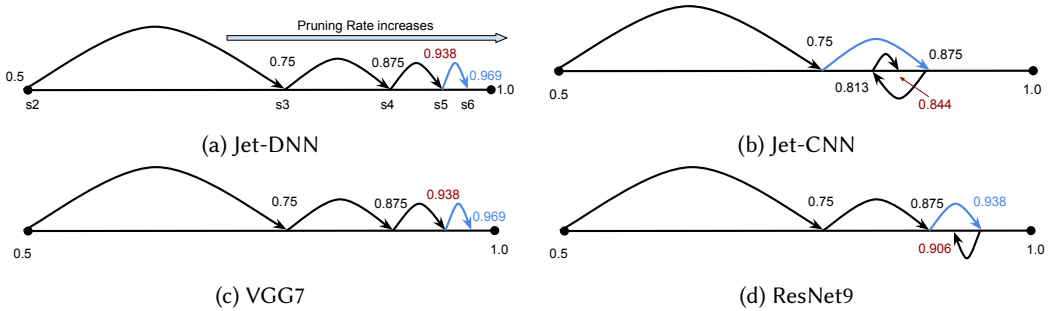


Fig. 9. The auto-pruning algorithm applied to models with binary search direction shown. Omitting step s_1 for visibility. The blue arrow indicates an accuracy loss $>$ user threshold; red denotes the optimal pruning rate.

5.2.2 Scaling strategy. To accommodate a large DNN design on an FPGA, we use the SCALING O -task that automatically reduces the layer size while tracking the accuracy loss α_s . The search stops either when the loss exceeds α_s . If necessary, α_s can be adjusted to achieve further size reduction with minimal impact on accuracy. This work sets α_s to 0.05%, which allows for model size reduction with negligible accuracy loss.

5.2.3 Quantization strategy. This section showcases the evaluation results of the quantization (Q) optimization applied to multiple DNN models within the hardware (HLS) optimization space.

Fig 11 shows the precision of the weights, biases and output of each virtual layer of the VGG7 model after being tuned by the quantization strategy with α_q set to 1%. Table 3 shows how the quantization affected key evaluation metrics relating to the performance and resource usage of 2 DNN designs. With α_q set to 1%, the proposed QHS quantization algorithm reduces DSP usage by a factor of 4.9 for the VGG7 model, and 8.5 for the JetDNN model. When α_q is increased to 5%, the designs are further compacted, but with a larger real accuracy loss. This table highlights how varying α_q levels affect model accuracy, DSP, LUT, and FF usage, illustrating the trade-offs between

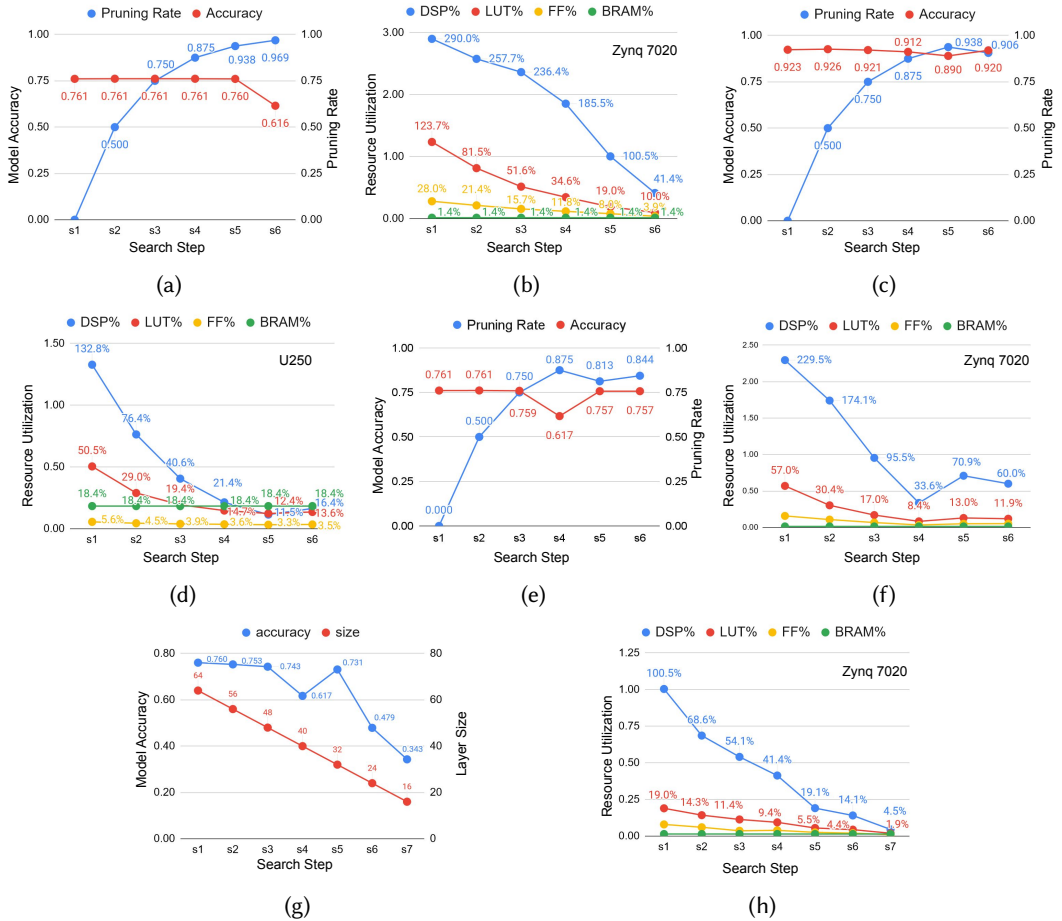


Fig. 10. (a) Pruning rates & accuracy of Jet-DNN. (b) Resource utilization of Jet-DNN design candidates after pruning. (c) Pruning rates & accuracy of ResNet9. (d) Resource utilization of ResNet9 design candidates after pruning. (e) Jet-DNN pruning rates & accuracy with scaling → pruning. (f) Resource utilization of Jet-DNN design candidates in (e). (g) Jet-DNN pruning rates & accuracy with pruning → scaling. (h) Resource utilization of Jet-DNN design candidates in (g).

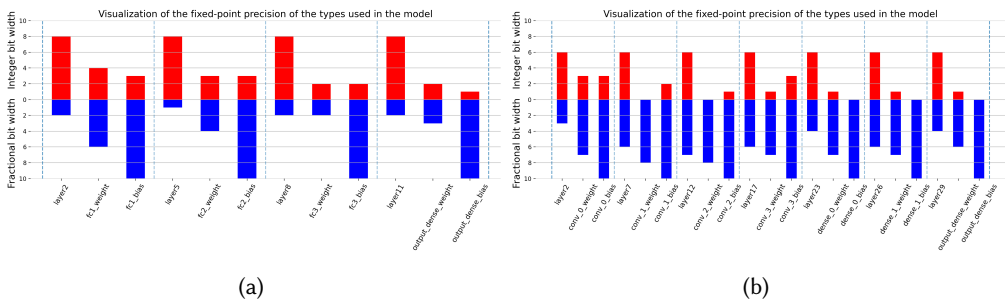


Fig. 11. (a) Quantized bitwidth of each layers in VGG7. (b) Quantized bitwidth of each layers in JetDNN.

Table 3. Results of designs with the quantization strategy using different α_q . VGG7 designs are using U250 while JetDNN designs are using Zynq 7020.

Model	α_q	DSP	LUT	FF	Acc
VGG7 Baseline	-	4568 (37.2%)	345k (20.0%)	65k (1.9%)	98.2%
VGG7 Quant.	0.01	934 (7.6%)	313k (18.1%)	51k (1.5%)	97.5%
VGG7 Quant.	0.05	505 (4.1%)	318k (18.4%)	66k (1.9%)	93.9%
JetDNN Baseline [28]	-	638 (290%)	66k (124%)	30k (28%)	76.1%
JetDNN Quant.	0.01	75 (34.1%)	57k (107%)	17k (16%)	75.5%
JetDNN Quant.	0.05	61 (27.7%)	76k (144%)	7.2k (6.8%)	71.6%

resource savings and accuracy as well as the effectiveness of the proposed QHS quantization algorithm.

5.3 Multiple O -task Strategies

With our framework, new strategies can be derived by building and revising a design-flow architecture. For instance, by inserting a scaling O -task before the pruning O -task in Fig. 8(a), a custom combined strategy can be created with results shown in Fig. 10(e) and (f). The new optimal pruning rate is 84.4% (Fig. 8(e)), lower than the previous 93.8% (Fig. 8(a)), due to reduced redundancy from the preceding scaling task. By switching the order of the O -tasks, a different optimization strategy performing pruning-then-scaling (pruning \rightarrow scaling) is achieved, resulting in a 0.7% accuracy drop after one scaling step, as seen in Fig. 10(g). Moreover, the three optimization O -tasks, pruning, scaling, and quantization, can be integrated into a single automated cross-stage strategy to enhance both performance and hardware efficiency, as illustrated in Fig. 8(c). We discuss the effects of different design-flow architectures with various combinations and orders in Section 5.7, and various tolerable loss in Section 5.8

5.4 Branching Flow

Fig. 12(a) illustrates a design flow that performs pruning for two alternate targets using the BRANCH K -task, for AMD/Xilinx FPGAs and Intel FPGAs. A user-defined selection function is supplied as a parameter to the BRANCH K -task which encodes a strategy determining the path forward for the design.

Fig. 13 presents the results of applying this design flow to an LSTM model on the MNIST dataset. Specifically, Fig. 13(a) illustrates the pruning rate and accuracy at each step using the PRUNING O -task. The tolerance is set to less than α_p (2%) in this design. Figs 13(b) and (c) show the resource utilization of the LSTM design after each pruning step respectively on an AMD KU115 FPGA and on an Intel A10 1150 FPGA. The DSP consumption is reduced from 6011 (108%) to 2101 (38.1%) on the AMD FPGA after the final pruning rate is optimized to be 71.9%. Compared to AMD's HLS compiler, which prefers DSP blocks, Intel's HLS compiler tends to favor the use of soft multipliers for implementation. As shown in Fig 13(c), most of the computation kernels are implemented using logic resources rather than DSP blocks.

While this design flow currently supports two types of FPGAs, it can be extended to include additional paths such as GPU, CPU and ASIC technologies. Moreover, this evaluation underscores the flexibility of our approach in utilizing the same software optimization task, specifically PRUNING, across multiple hardware targets.

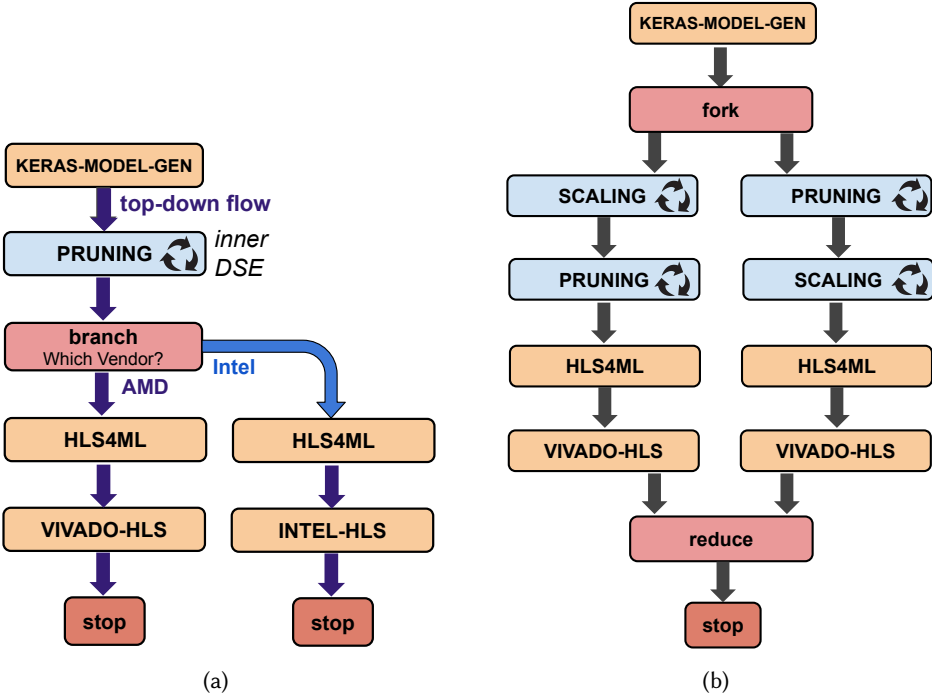


Fig. 12. (a) Pruning optimization targeting different vendors using the BRANCH K -task; (b) Combined strategy of scaling and pruning, exploring the order of O -tasks.

5.5 Parallel Flow

Our framework enables the execution of multiple optimization paths in parallel, allowing the selection of the best outcome among them. In Fig. 12(b), we show a design-flow with two parallel paths, where the execution order of two O -tasks is changed: scaling \rightarrow pruning and pruning \rightarrow scaling. To support parallel branches, we use the FORK task to connect multiple strategy paths. The results from each path are then evaluated based on predefined criteria, such as accuracy or resource utilization, using the REDUCE task. For this strategy, a Pareto analysis was performed on the designs resulting from both paths, as shown in Fig. 14. By employing this design-flow, designers can explore various optimization combinations and sequences when the outcomes of these strategies are not clear.

5.6 Bottom-up Flow

Fig 15 reveal two distinct flows in the optimization strategies: top-down, where information flows from the DNN to the hardware stage, and bottom-up, the reverse. We have automated both flows by customizing the K -task BRANCH with a user-defined predicate function to activate or stop the bottom-up flow if the resulting design overmaps. The BRANCH task also support a user-supplied action function that is triggered when the predicate condition is true. For our current strategies, the action function changes the CFG section of the meta-model, increasing the accuracy tolerance parameters α_p , α_s , and α_q (if applicable) for the next iteration. Note that our current strategies in Fig. 15 have two DSE loops: an inner-loop that is codified within each O -task and an outer-loop supported by the bottom-up flow. Users can develop more complex strategies by customizing the outer loop, for instance, by updating the bottom-up condition and parameter tuning.

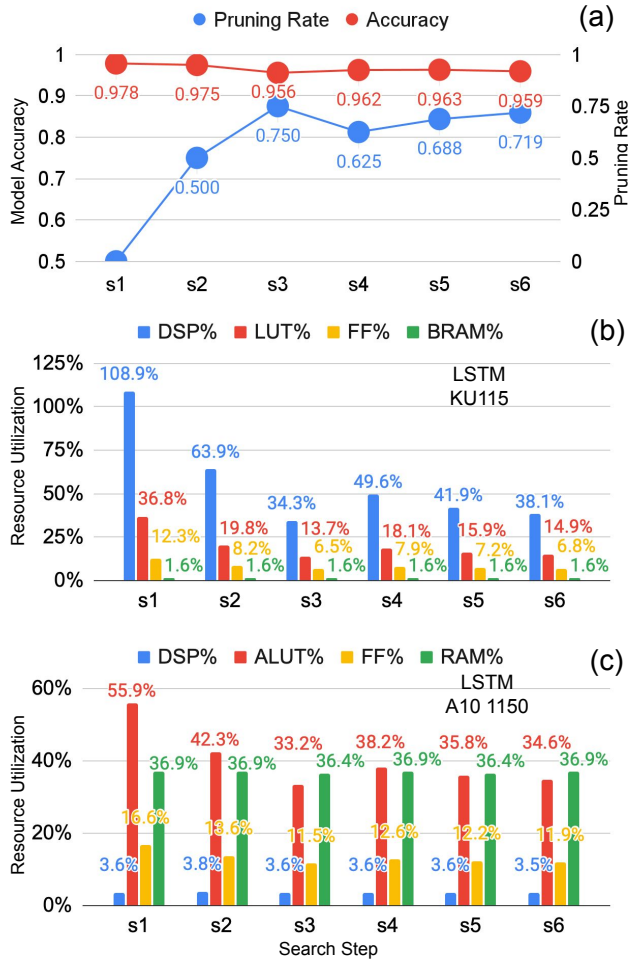


Fig. 13. LSTM model optimization on two FPGA platforms: (a) pruning rate and model accuracy using the PRUNING *O*-task; (b) resource utilization on an AMD KU115 FPGA; (c) resource utilization on an Intel A10 1150 FPGA.

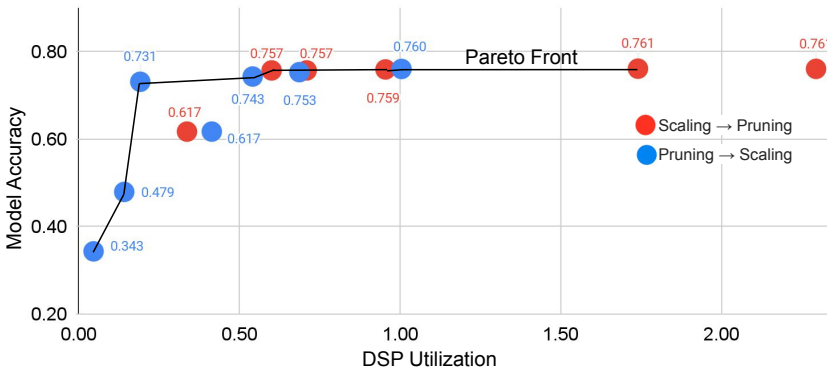


Fig. 14. Pareto Front meta-model designs post REDUCE *K*-task, color-coded paths.

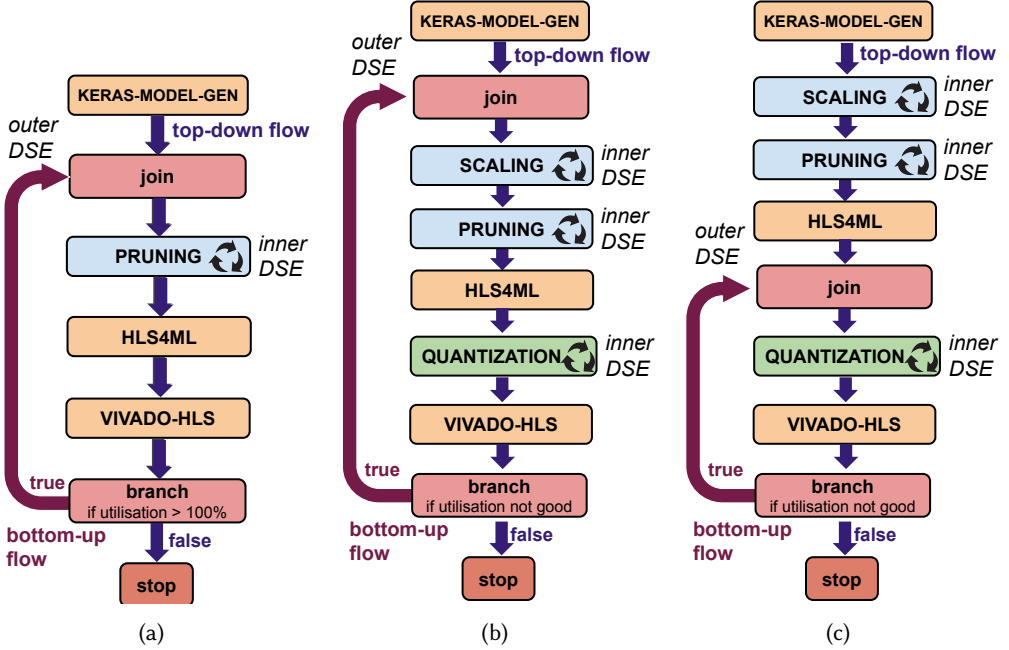


Fig. 15. (a) Pruning strategy with Branch. (b) Combined strategy with Branch to python (SW) space. (c) The combined strategy with Branch to HLS space.

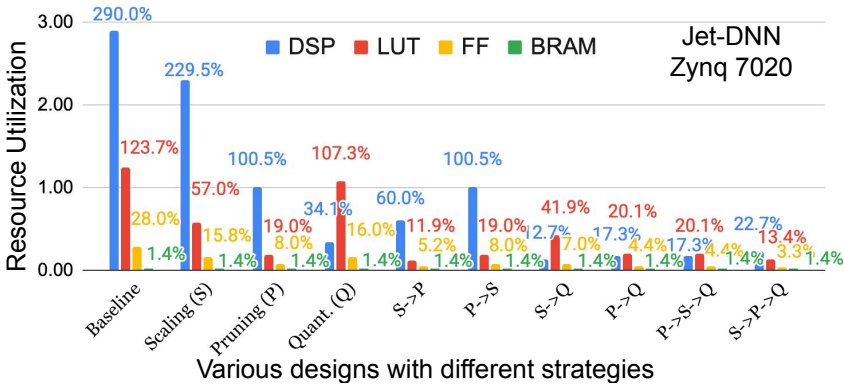
5.7 Combination and Order

Combining optimization methods increases diversity and potential designs, improving optimal balance between accuracy and efficiency. We systematically evaluate all candidates combined optimization strategies based on our current set of 3 optimization tasks, Scaling (S), Pruning (P), and Quantization (Q), to identify the most effective combination and order. The α_p , α_s and α_q are set to 2%, 0.05% and 1%. In particular, Fig 16(a) shows the hardware resource utilization results after each strategy and Fig 17 shows the corresponding latency, initiation interval and model accuracy. The final optimized model of Jet-DNN after scaling, pruning and quantization is depicted as “S→P→Q” design, resulting in a reduction of the DSP usage by around 92% and LUT usage by around 89% compared with the original design (baseline [7, 28]). In addition, the latency is reduced by 35% while the accuracy loss is trivial, as shown in Fig 17. The same search is performed on the VGG7 network with results shown in Fig. 16(b). The final design reduces DSP usage by a factor of 23 with the same latency and around 1.1% accuracy loss compared with the baseline design.

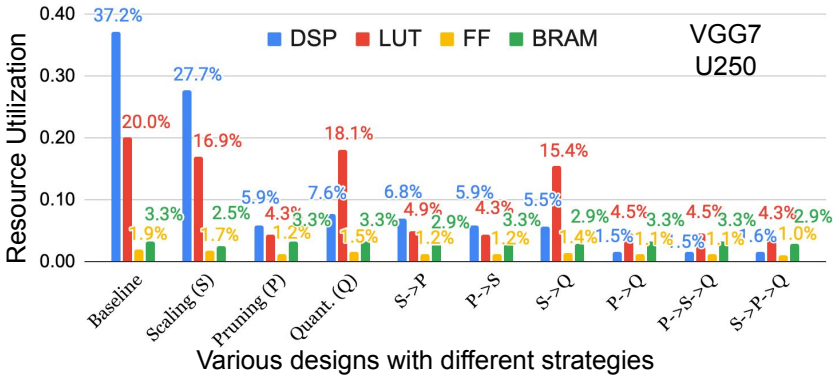
The search for optimal combinations and sequences with multiple O-tasks can be computationally demanding due to the exponential growth of the search space with the number of O-tasks. Advanced search methods can replace the current brute-force search. Recent studies [9, 19, 46] demonstrate surrogate models can expedite the search. Our framework facilitates the deployment of such techniques, enabling users to interface a search algorithm with the hardware design with minimal programming effort.

5.8 Tolerable Loss Variation

This subsection evaluate the performance and efficiency trade-offs when using different values for the maximum tolerable accuracy loss (α_p , α_s and α_q) for each optimization task to determine the effectiveness of their combination. We compare three strategies: Q, S→Q, and S→P→Q, using Grid Search to create a Pareto frontier by assessing model accuracy against DSP and LUT utilization. As



(a)



(b)

Fig. 16. (a) The hardware resources and latency of the Jet-DNN designs after various strategies. (b) The hardware resources and latency of the VGG7 designs after various strategies.

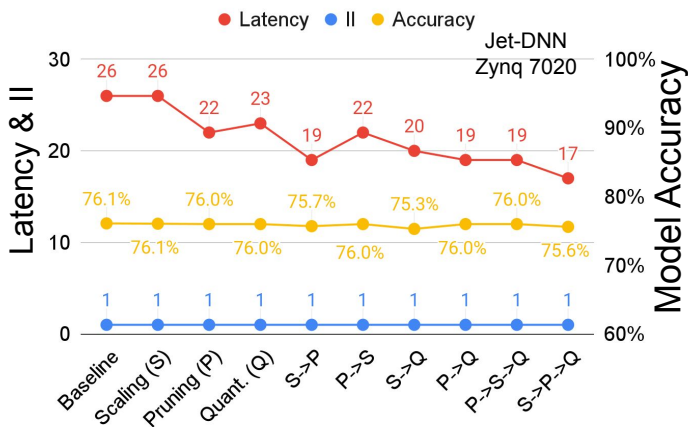


Fig. 17. Latency, Initiation Interval (II) and model accuracy of various designs with different strategies

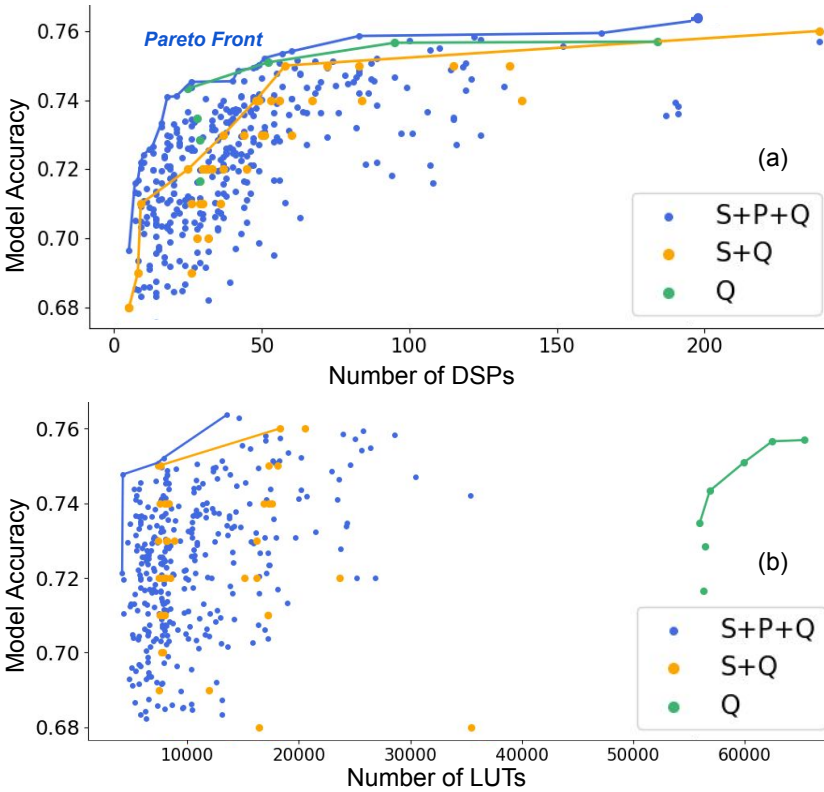


Fig. 18. Comparison of Pareto frontiers of **JetDNN** model accuracy and resource utilization using different optimization strategies.

illustrated in Fig. 18, our findings reveal that the **S**→**P**→**Q** strategy outperforms both the **S**→**Q** and **Q** strategies across multiple dimensions, including accuracy, DSP and LUT usage. However, it is important to note that the **S**→**P**→**Q** strategy is less efficient in terms of time and design space requirements, demanding 220.5 times more time than the **Q** strategy. Practical applications may require a balance between performance, hardware resource utilization, and time investment, with the choice of strategy complexity and design space contingent on the specific use case. Our following experiments in this paper build on these findings, focusing on the **S**→**P**→**Q** strategy.

5.9 Design-Space Exploration Strategies

Finding the optimal designs with grid search is time-consuming, as discussed in the previous section. This section investigates various DSE algorithms, including grid search, stochastic grid search (SGS), and Bayesian optimization. Fig. 19 presents the results. Each colored dot represents a design at a specific iteration, with different colors indicating different algorithms. The solid lines represent the Pareto Frontier of each algorithm over iterations, with each colored line corresponding to 22 iterations taking 40 hours. The uppermost grey line indicates a total of 343 iterations using extensive grid search over 624 hours, representing a baseline for comparison. The Bayesian optimization achieves similar results with just 22 iterations, significantly reducing processing time by a factor of 15.6 compared to Grid Search. Compared to SGS, Bayesian optimization’s efficient parameter search yields multiple points near the Pareto frontier, indicating its effectiveness in finding optimal designs and approaching global optima. This effective parameter search by employing past results

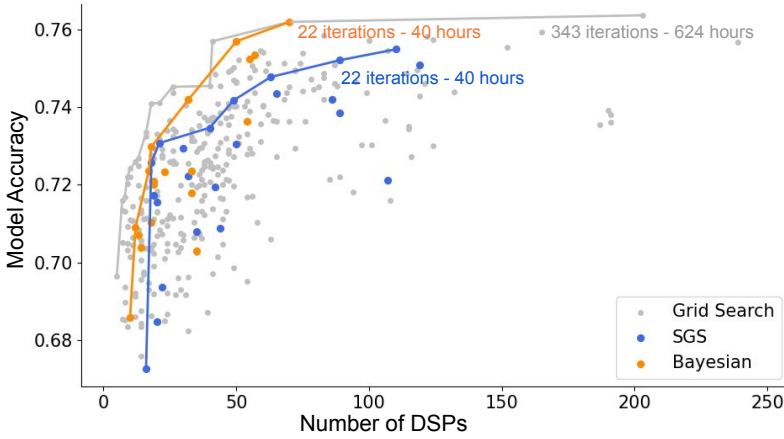


Fig. 19. DSP-Accuracy Pareto frontiers for each optimization using different DSE methods for **JetDNN** models.

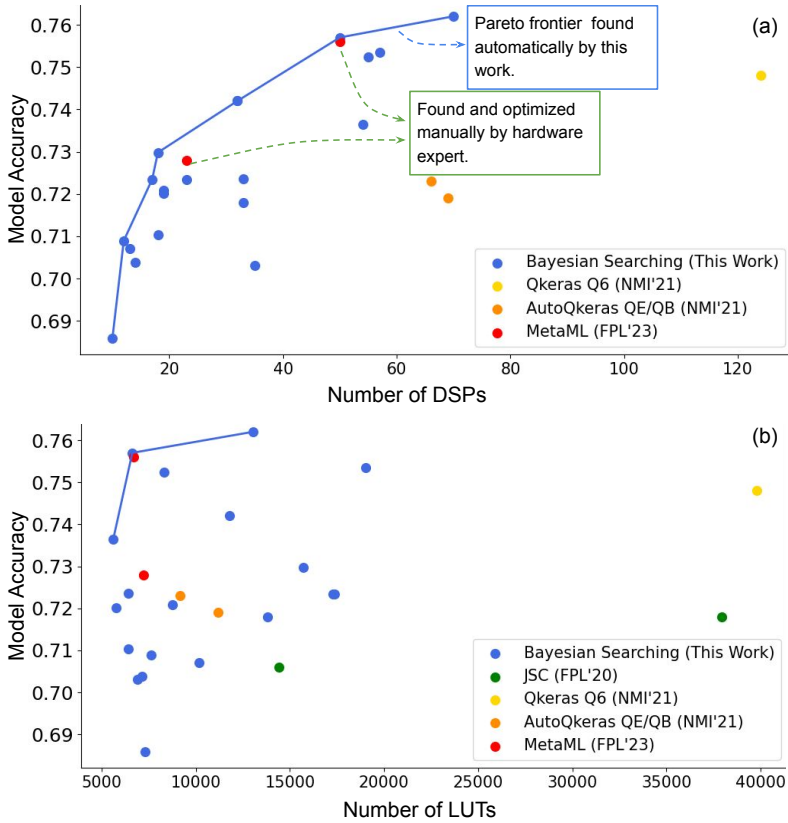


Fig. 20. Comparison of resource utilization of the FPGA-based **JetDNN** networks using our approach and others (LogicNets JSC [39], Qkeras Q6 [5], AutoQkeras QE/QB [5] and MetaML [28]) on an AMD/Xilinx VU9P FPGA. The Pareto frontier is highlighted.

Table 4. Performance comparison with the FPGA designs of Jet-DNN network using other approaches on Xilinx FPGAs with a clock frequency of 200MHz.

Model	$\alpha_s, \alpha_p, \alpha_q$ (%)	FPGA	Acc.(%)	Lat. (ns)	DSP (%)	LUT (%)
HLS4ML Jet-DNN [7]	-	KU115	75	75	954 (17.3)	-
FPL'20 LogicNets JSC-M [39]	-	VU9P	70.6	NA	0 (0)	14,428 (1.2)
FPL'20 LogicNets JSC-L [39]	-	VU9P	71.8	13 ^a	0 (0)	37,931 (3.2)
NMI'21 [5] Qkeras Q6	-	VU9P	74.8	55	124 (1.8)	39,782 (3.4)
NMI'21 [5] AutoQkeras QE	-	VU9P	72.3	55	66 (1.0)	9,149 (0.8)
NMI'21 [5] AutoQkeras QB	-	VU9P	71.9	70	69 (1.0)	11,193 (0.9)
PL'23 [28] MetaML	-	VU9P	76.1	70	638 (9.3)	69,751 (5.9)
FPL'23 [28] MetaML	{0.05, 2, 1}	VU9P	75.6	45	50 (0.7)	6,698 (0.6)
FPL'23 [28] MetaML	{0.05, 2, 4}	VU9P	72.8	40	23 (0.2)	7,224 (0.6)
This work (Best Acc.)	{0.5, 0.1, 0.1}	VU9P	76.2	55	272 (4.0)	14,580 (1.2)
This work (Best DSP)	{0.5, 3, 4}	VU9P	69.7	40	5 (0.1)	9,026 (0.8)
This work (Best LUT)	{2, 5, 1}	VU9P	72.1	45	47 (0.7)	4,410 (0.4)
This work ^b (Acc.-DSP-LUT)	{0.5, 2, 0.5}	VU9P	76.1	50	70 (1.0)	13,042 (1.1)
This work ^b (Acc.-DSP-LUT)	{4, 0.5, 0.5}	VU9P	75.7	45	50 (0.7)	6,634 (0.6)
This work ^c (Acc.-LUT)	{4, 4, 0.5}	VU9P	73.7	45	54 (0.8)	5,624 (0.5)
This work ^d (Acc.-DSP)	{2, 3, 4}	VU9P	70.9	40	12 (0.2)	7,637 (0.8)

^a A clock frequency of 384 MHz is used and the final softmax layer is removed.

^b On both Accuracy-DSP and Accuracy-LUT Pareto lines as shown in Fig 20.

^c Only on Accuracy-LUT Pareto line. ^d Only on Accuracy-DSP Pareto line.

demonstrates the robustness of the Bayesian optimization approach, enabling users to optimize models while minimizing time and effort.

5.10 Discussion and Comparison

Our evaluation results indicate that our combined O -task optimization strategy typically outperforms single O -task techniques. Furthermore, the order in which these optimization techniques are applied plays a crucial role, as different orders produce varying final results, as depicted in Fig. 16.

To highlight the advantages of our framework, we compare our results to those from other approaches targeting low-latency, low-resource, fully unfolded FPGA implementation of the JetDNN network, including LogicNets [39] JSC-M and JSC-L, QKeras-based Q6 [5], AutoQKeras-based QE and QB [5], and MetaML [28] in Fig. 20 and Table 4. All designs use the same architecture, except for JSC-L, which employs a larger architecture.

Compared to original Jet-DNN [7], our design achieves higher accuracy (up to 76.2%) while using less hardware resources. When compared with LogicNets JSC-M and JSC-L [39], which achieve accuracies of 70.6% and 71.8% respectively, our design demonstrates up to 5.6% higher accuracy while also offering resource efficiency. Against the AutoQkeras Q6 and QE designs [5], which yield accuracies of 74.8% and 72.3% respectively, our framework attains higher accuracy and lower latency while providing more granular trade-offs between resource utilization and latency. Compared to MetaML [28] with manual optimization, our work achieves comparable or better accuracy across various configurations with automatic optimization. Overall, the versatility of

our design, which balances accuracy, latency, and resource utilization across different objectives, highlights its superiority and adaptability for diverse FPGA-based DNN applications.

This effective parameter search demonstrates the robustness of the Bayesian Optimization approach, enabling users to optimize models while minimizing development time. Besides, this work demonstrates flexibility and effectiveness by achieving competitive performance across multiple configurations, highlighting its adaptability to different optimization priorities such as Accuracy, DSP and LUT. It is worth noting that our results are identified automatically while the other approaches involve manual optimization by DNN and hardware experts.

6 CONCLUSION

This paper presents a novel co-optimization framework for FPGA-based DNN accelerators, which comprises building blocks that facilitate rapid development of customized cross-stage design flows, automating the entire design iteration process. The results demonstrate that our approach significantly reduces DSP resource usage by up to 92% and LUT usage by up to 89%, while maintaining accuracy and without requiring human effort or domain expertise. In addition, our results reveal that Bayesian optimization in DSE significantly streamlines the process, achieving results comparable to grid search but with a 15.6-fold reduction in processing time. Future work will extend this approach to include RTL space, support more DNN architectures, including Variational Autoencoder (VAE) [26] and transformer [45] networks, and incorporate more optimization strategies like balancing initiation interval [30, 33] for further improvements in hardware efficiency and model performance.

Acknowledgement: The support of the United Kingdom EPSRC (grant number UKRI256, EP/V028251/1, EP/N031768/1, EP/S030069/1, and EP/X036006/1), Intel, and AMD is gratefully acknowledged. We thank Markus Rognlien, Shuo Liu and Anyan Zhao for their help.

REFERENCES

- [1] 2023. OpenVINO toolkit. <https://github.com/openvinotoolkit/openvino>.
- [2] Mohamed S Abdelfattah, Lukasz Dudziak, Thomas Chau, Royson Lee, Hyeji Kim, and Nicholas D Lane. 2020. Best of both worlds: Automl codesign of a cnn and its hardware accelerator. In *2020 57th ACM/IEEE Design Automation Conference (DAC)*. IEEE, 1–6.
- [3] Nicolas Bohm Agostini, Serena Curzel, Vinay Amatya, Cheng Tan, Marco Minutoli, Vito Giovanni Castellana, Joseph Manzano, David Kaeli, and Antonino Tumeo. 2022. An MLIR-based Compiler Flow for System-Level Design and Hardware Acceleration. In *Proceedings of the 41st IEEE/ACM International Conference on Computer-Aided Design*. 1–9.
- [4] Tianqi Chen, Thierry Moreau, Ziheng Jiang, Lianmin Zheng, Eddie Yan, Haichen Shen, Meghan Cowan, Leyuan Wang, Yuwei Hu, Luis Ceze, et al. 2018. {TVM}: An automated {End-to-End} optimizing compiler for deep learning. In *13th USENIX Symposium on Operating Systems Design and Implementation (OSDI 18)*. 578–594.
- [5] Claudionor N Coelho, Aki Kuusela, Shan Li, Hao Zhuang, Jennifer Ngadiuba, Thea Klaeboe Aarrestad, Vladimir Loncar, Maurizio Pierini, Adrian Alan Pol, and Sioni Summers. 2021. Automatic heterogeneous quantization of deep neural networks for low-latency inference on the edge for particle detectors. *Nature Machine Intelligence* 3, 8 (2021), 675–686.
- [6] Zhen Dong, Yizhao Gao, Qijing Huang, John Wawrzyniek, Hayden KH So, and Kurt Keutzer. 2021. Hao: Hardware-aware neural architecture optimization for efficient inference. In *2021 IEEE 29th Annual International Symposium on Field-Programmable Custom Computing Machines (FCCM)*. IEEE, 50–59.
- [7] Javier Duarte, Song Han, Philip Harris, Sergo Jindariani, Edward Kreinar, Benjamin Kreis, Jennifer Ngadiuba, Maurizio Pierini, Ryan Rivera, Nhan Tran, et al. 2018. Fast inference of deep neural networks in FPGAs for particle physics. *Journal of Instrumentation* 13, 07 (2018), P07027.
- [8] Hongxiang Fan, Martin Ferianc, Zhiqiang Que, He Li, Shuanglong Liu, Xinyu Niu, and Wayne Luk. 2022. Algorithm and hardware co-design for reconfigurable cnn accelerator. In *2022 27th Asia and South Pacific Design Automation Conference (ASP-DAC)*. IEEE, 250–255.
- [9] Lorenzo Ferretti, Andrea Cini, Georgios Zacharopoulos, Cesare Alippi, and Laura Pozzi. 2022. Graph Neural Networks for High-Level Synthesis Design Space Exploration. *ACM Transactions on Design Automation of Electronic Systems* 28, 2 (2022), 1–20.

- [10] Fumio Hamanaka, Takashi Odan, Kenji Kise, and Thiem Van Chu. 2023. An Exploration of State-of-the-art Automation Frameworks for FPGA-based DNN Acceleration. *IEEE Access* (2023).
- [11] Cong Hao and Deming Chen. 2018. Deep neural network model and FPGA accelerator co-design: Opportunities and challenges. In *2018 14th IEEE International Conference on Solid-State and Integrated Circuit Technology (ICSICT)*. IEEE, 1–4.
- [12] Cong Hao, Yao Chen, Xinheng Liu, Atif Sarwari, Daryl Sew, Ashutosh Dhar, Bryan Wu, Dongdong Fu, Jinjun Xiong, Wen-mei Hwu, et al. 2019. NAI: Neural architecture and implementation search and its applications in autonomous driving. In *2019 IEEE/ACM International Conference on Computer-Aided Design (ICCAD)*. IEEE, 1–8.
- [13] Cong Hao, Yao Chen, Xiaofan Zhang, Yuhong Li, Jinjun Xiong, Wen-mei Hwu, and Deming Chen. 2020. Effective algorithm-accelerator co-design for ai solutions on edge devices. In *Proceedings of the 2020 on Great Lakes Symposium on VLSI*. 283–290.
- [14] Cong Hao, Jordan Dotzel, Jinjun Xiong, Luca Benini, Zhiru Zhang, and Deming Chen. 2021. Enabling design methodologies and future trends for edge AI: specialization and codesign. *IEEE Design & Test* 38, 4 (2021), 7–26.
- [15] Cong Hao, Xiaofan Zhang, Yuhong Li, Sitao Huang, Jinjun Xiong, Kyle Rupnow, Wen-mei Hwu, and Deming Chen. 2019. FPGA/DNN co-design: An efficient design methodology for 1ot intelligence on the edge. In *2019 56th ACM/IEEE Design Automation Conference (DAC)*. IEEE, 1–6.
- [16] Kaïming He, Xiangyu Zhang, Shaoqing Ren, and Jian Sun. 2016. Deep residual learning for image recognition. In *Proceedings of the IEEE conference on computer vision and pattern recognition*. 770–778.
- [17] Weiwen Jiang, Lei Yang, Edwin Hsing-Mean Sha, Qingfeng Zhuge, Shouzhen Gu, Sakyasingha Dasgupta, Yiyu Shi, and Jingtong Hu. 2020. Hardware/software co-exploration of neural architectures. *IEEE Transactions on Computer-Aided Design of Integrated Circuits and Systems* 39, 12 (2020), 4805–4815.
- [18] Vinod Kathail. 2020. Xilinx vitis unified software platform. In *Proceedings of the 2020 ACM/SIGDA International Symposium on Field-Programmable Gate Arrays*. 173–174.
- [19] Maciej Kurek, Marc Peter Deisenroth, Wayne Luk, and Timothy Todman. 2016. Knowledge transfer in automatic optimisation of reconfigurable designs. In *2016 IEEE 24th Annual International Symposium on Field-Programmable Custom Computing Machines (FCCM)*. IEEE, 84–87.
- [20] Yann LeCun, Yoshua Bengio, and Geoffrey Hinton. 2015. Deep learning. *nature* 521, 7553 (2015), 436–444.
- [21] Yann LeCun, Léon Bottou, Yoshua Bengio, and Patrick Haffner. 1998. Gradient-based learning applied to document recognition. *Proc. IEEE* 86, 11 (1998), 2278–2324.
- [22] Atefeh Mehrabi, Aninda Manocha, Benjamin C Lee, and Daniel J Sorin. 2020. Bayesian optimization for efficient accelerator synthesis. *ACM Transactions on Architecture and Code Optimization (TACO)* 18, 1 (2020), 1–25.
- [23] Eric A Moreno, Olmo Cerri, Javier M Duarte, Harvey B Newman, Thong Q Nguyen, Avikar Periwal, Maurizio Pierini, Aidana Serikova, Maria Spiropulu, and Jean-Roch Vlimant. 2020. JEDI-net: a jet identification algorithm based on interaction networks. *The European Physical Journal C* 80, 1 (2020), 1–15.
- [24] Yuval Netzer, Tao Wang, Adam Coates, Alessandro Bissacco, Bo Wu, and Andrew Y Ng. 2011. Reading digits in natural images with unsupervised feature learning. (2011).
- [25] Jonas Ney, Dominik Loroeh, Vladimir Rybalkin, Nico Weber, Jens Krüger, and Norbert Wehn. 2021. HALF: Holistic auto machine learning for FPGAs. In *2021 31st International Conference on Field-Programmable Logic and Applications (FPL)*. IEEE, 363–368.
- [26] Zhiqiang Que et al. 2024. Low Latency Variational Autoencoder on FPGAs. *IEEE Journal on Emerging and Selected Topics in Circuits and Systems* (2024).
- [27] Zhiqiang Que, Jose GF Coutinho, and Wayne Luk. 2024. Deep Learning Design-Flow with Static and Dynamic Optimizations. In *2024 IEEE 17th International Conference on Solid-State & Integrated Circuit Technology (ICSICT)*. IEEE, 1–4.
- [28] Zhiqiang Que, Shuo Liu, Markus Rognlien, Ce Guo, Jose GF Coutinho, and Wayne Luk. 2023. MetaML: Automating Customizable Cross-Stage Design-Flow for Deep Learning Acceleration. In *2023 30th International Conference on Field-Programmable Logic and Applications (FPL)*. IEEE.
- [29] Zhiqiang Que, Hiroki Nakahara, Eriko Nurvitadhi, Hongxiang Fan, Chenglong Zeng, Jiuxi Meng, Xinyu Niu, and Wayne Luk. 2020. Optimizing Reconfigurable Recurrent Neural Networks. In *IEEE 28th Annual International Symposium on Field-Programmable Custom Computing Machines (FCCM)*. IEEE, 10–18.
- [30] Zhiqiang Que, Erwei Wang, Umar Marikar, Eric Moreno, Jennifer Ngadiuba, Hamza Javed, Bartłomiej Borzyszkowski, Thea Aarrestad, Vladimir Loncar, Sioni Summers, et al. 2021. Accelerating recurrent neural networks for gravitational wave experiments. In *2021 IEEE 32nd International Conference on Application-specific Systems, Architectures and Processors (ASAP)*. IEEE, 117–124.
- [31] Zhiqiang Que, Anyan Zhao, Jose GF Coutinho, Ce Guo, and Wayne Luk. 2024. Optimizing DNN Accelerator Compression Using Tolerable Accuracy Loss. In *International conference on field-programmable technology (FPT)*. IEEE.

- [32] Brandon Reagen, José Miguel Hernández-Lobato, Robert Adolf, Michael Gelbart, Paul Whatmough, Gu-Yeon Wei, and David Brooks. 2017. A case for efficient accelerator design space exploration via bayesian optimization. In *2017 IEEE/ACM International Symposium on Low Power Electronics and Design (ISLPED)*. IEEE, 1–6.
- [33] Markus Rognlien, Zhiqiang Que, Jose GF Coutinho, and Wayne Luk. 2022. Hardware-aware optimizations for deep learning inference on edge devices. In *International Symposium on Applied Reconfigurable Computing*. Springer, 118–133.
- [34] Karen Simonyan and Andrew Zisserman. 2014. Very deep convolutional networks for large-scale image recognition. *arXiv preprint arXiv:1409.1556* (2014).
- [35] Atefeh Sohrabzadeh, Yunsheng Bai, Yizhou Sun, and Jason Cong. 2022. Automated accelerator optimization aided by graph neural networks. In *Proceedings of the 59th ACM/IEEE Design Automation Conference*. 55–60.
- [36] Vivienne Sze, Yu-Hsin Chen, Tien-Ju Yang, and Joel S Emer. 2017. Efficient processing of deep neural networks: A tutorial and survey. *Proc. IEEE* 105, 12 (2017), 2295–2329.
- [37] Stephen Tridgell, Martin Kumm, Martin Hardieck, David Boland, Duncan Moss, Peter Zipf, and Philip HW Leong. 2019. Unrolling Ternary Neural Networks. *ACM Transactions on Reconfigurable Technology and Systems (TRETS)* 12, 4 (2019), 1–23.
- [38] Shikhar Tuli, Chia-Hao Li, Ritvik Sharma, and Niraj K Jha. 2023. CODEBench: A neural architecture and hardware accelerator co-design framework. *ACM Transactions on Embedded Computing Systems* 22, 3 (2023), 1–30.
- [39] Yaman Umuroglu, Yash Akhauri, Nicholas James Fraser, and Michaela Blott. 2020. LogicNets: co-designed neural networks and circuits for extreme-throughput applications. In *2020 30th International Conference on Field-Programmable Logic and Applications (FPL)*. IEEE, 291–297.
- [40] Yaman Umuroglu, Nicholas J Fraser, Giulio Gambardella, Michaela Blott, Philip Leong, Magnus Jahre, and Kees Vissers. 2017. FINN: A framework for fast, scalable binarized neural network inference. In *Proceedings of the 2017 ACM/SIGDA international symposium on field-programmable gate arrays*. 65–74.
- [41] Jessica Vandebon, Jose G. F. Coutinho, Wayne Luk, and Eriko Nurvitadhi. 2021. Enhancing High-Level Synthesis Using a Meta-Programming Approach. *IEEE Trans. Comput.* 70, 12 (2021), 2043–2055. <https://doi.org/10.1109/TC.2021.3096429>
- [42] Jessica Vandebon, Jose G. F. Coutinho, Wayne Luk, Eriko Nurvitadhi, and Tim Todman. 2020. Artisan: a Meta-Programming Approach For Codifying Optimisation Strategies. In *2020 IEEE 28th Annual International Symposium on Field-Programmable Custom Computing Machines (FCCM)*.
- [43] Stylianos I Venieris and Christos-Savvas Bouganis. 2016. fpgaConvNet: A framework for mapping convolutional neural networks on FPGAs. In *2016 IEEE 24th Annual International Symposium on Field-Programmable Custom Computing Machines (FCCM)*. IEEE, 40–47.
- [44] Erwei Wang, James J Davis, Ruizhe Zhao, Ho-Cheung Ng, Xinyu Niu, Wayne Luk, Peter YK Cheung, and George A Constantinides. 2019. Deep neural network approximation for custom hardware: Where we’ve been, where we’re going. *ACM Computing Surveys (CSUR)* 52, 2 (2019), 1–39.
- [45] Filip Wojcicki, Zhiqiang Que, Alexander D Tapper, and Wayne Luk. 2022. Accelerating transformer neural networks on fpgas for high energy physics experiments. In *2022 International Conference on Field-Programmable Technology (ICFPT)*. IEEE, 1–8.
- [46] Nan Wu, Yuan Xie, and Cong Hao. 2021. Ironman: GNN-assisted design space exploration in high-level synthesis via reinforcement learning. In *Proceedings of the 2021 on Great Lakes Symposium on VLSI*. 39–44.
- [47] Pengfei Xu, Xiaofan Zhang, Cong Hao, Yang Zhao, Yongan Zhang, Yue Wang, Chaojian Li, Zetong Guan, Deming Chen, and Yingyan Lin. 2020. AutoDNNchip: An automated DNN chip predictor and builder for both FPGAs and ASICs. In *Proceedings of the 2020 ACM/SIGDA International Symposium on Field-Programmable Gate Arrays*. 40–50.
- [48] Yifan Yang, Qijing Huang, Bichen Wu, Tianjun Zhang, Liang Ma, Giulio Gambardella, Michaela Blott, Luciano Lavagno, Kees Vissers, John Wawrzynek, et al. 2019. Synetgy: Algorithm-hardware co-design for convnet accelerators on embedded fpgas. In *Proceedings of the 2019 ACM/SIGDA international symposium on field-programmable gate arrays*. 23–32.
- [49] Hanchen Ye, Cong Hao, Jianyi Cheng, Hyunmin Jeong, Jack Huang, Stephen Neuendorffer, and Deming Chen. 2022. Scalehls: A new scalable high-level synthesis framework on multi-level intermediate representation. In *2022 IEEE International Symposium on High-Performance Computer Architecture (HPCA)*. IEEE, 741–755.
- [50] Chen Zhang, Peng Li, Guangyu Sun, Yijin Guan, Bingjun Xiao, and Jason Cong. 2015. Optimizing FPGA-based accelerator design for deep convolutional neural networks. In *Proceedings of the 2015 ACM/SIGDA international symposium on field-programmable gate arrays*. 161–170.
- [51] Xiaofan Zhang, Yuhong Li, Junhao Pan, and Deming Chen. 2022. Algorithm/Accelerator Co-Design and Co-Search for Edge AI. *IEEE Transactions on Circuits and Systems II: Express Briefs* 69, 7 (2022), 3064–3070.
- [52] Xiaofan Zhang, Hanchen Ye, Junsong Wang, Yonghua Lin, Jinjun Xiong, Wen-mei Hwu, and Deming Chen. 2020. DNNExplorer: a framework for modeling and exploring a novel paradigm of FPGA-based DNN accelerator. In *Proceedings of the 39th International Conference on Computer-Aided Design*. 1–9.